Supporting Information for

Multiple modulation of hierarchical NiS$_2$ nanosheets by Mn heteroatom doping engineering for boosting alkaline and neutral hydrogen evolution

Lingyou Zeng, Zhi Liu, Kaian Sun, Yanju Chen, Jinchong Zhao, Yinjuan Chen, Yuan Pan,* Yukun Lu, Yunqi Liu* and Chenguang Liu

State Key Laboratory of Heavy Oil Processing, Key Laboratory of Catalysis, China University of Petroleum (East China), Qingdao, 266580, P. R. China. E-mail: panyuan@upc.edu.cn; liuyq-group@upc.edu.cn

The supporting information includes two sections:

I Experimental and Computational Details

II Additional Figures and Tables

I Experimental Details

I.1 Materials and Reagents. Ni foam was purchased from Changsha Lyrun Mater. Co. Ltd. All the reagents were of analytical grade and used as received from Aladdin Chemical Co. Ltd. without further purification.

I.2 Preparation of hydroxide precursor/NF. Commercial Ni foams were rinsed with acetone for 5 min, then sonicated in 3 M HCl for 10 min, and finally washed with ethanol and distilled water. The acetone was used to clean the oil stains, and the HCl solution was used to remove the surface oxide species (e.g., NiO) on the Ni foam surface. To synthesis hydroxide precursor/NF, a given amount (2 mmol total) of $Ni(NO_3)_2 \cdot 6H_2O$, $MnSO_4 \cdot H_2O$, 4 mmol NH_4F, and 10 mmol urea were dissolved in 40 mL water and stirred for 10 min at room temperature. The solution was transferred into a 50 mL Teflon-lined autoclave and a piece of fresh-treated Ni foam (1 cm × 2.5 cm) was put into the solution. The autoclave was then sealed and heated at 120°C for 6 h in an electric oven. After the autoclave was cooled down to room temperature naturally, the Mn-Ni hydroxide loaded NF was taken out, rinsed with water and ethanol, and dried in a vacuum oven at 30°C for 12 h. The feed mole ratio of $Ni(NO_3)_2 \cdot 6H_2O$ and $MnSO_4 \cdot H_2O$ (2 mmol total) were varied to synthesize samples with different Mn/Ni ratios (Table S1).

I.3 Preparation of the Mn-doped NiS$_2$ nanosheet/NF. The hydroxide precursor/NF and 0.5 g S were put at two separate positions in a ceramic boat inside a tube furnace with S at the upstream of the furnace. Subsequently, the furnace was heated at 300 °C for 1 h in Ar atmosphere, and then naturally cooled down to ambient temperature. The loading mass of sulfide catalyst on NF was about 1.15 mg cm^{-2}. Bare NiS_2/NF was also prepared from its hydroxide grown on Ni foam without the presence of Mn salt.

I.4 Material Characterization. XRD patterns were performed in X′Pert PRO MPD system with a Cu Kα source. ICP-AES analysis was performed on Model Agilent 720. SEM images were carried out in a Hitachi S-4800 accelerating voltage of 15 kV. High resolution TEM and SAED were collected with JEOL-2100F system working at 200 kV. XPS measurements were carried out using an AMICUS ESCA 3400 with Kα radiation. Ni and Mo K-edge XAFS spectra

were measured at 1W1B station in BSRF (Beijing Synchrotron Radiation Facility, P. R. China) operated at 2.5 GeV with the maximum current of 250 mA.

I.5 Electrochemical Measurement. Electrochemical measurements were carried out on an electrochemical workstation (CHI 600E, CH Instruments Inc.) with a standard three-electrode configuration using the self-supported catalysts as the working electrode, Au foil and Ag/AgCl electrode as the counter electrode and the reference electrode, respectively. For comparison, the working electrode of the commercial Pt/C catalyst was fabricated by ultrasonicating Pt/C (20 wt.% Pt) powder in ethanol solution with Nafion ionomer (Sigma-Aldrich) followed by coating the catalyst ink on a piece of Ni foam (1 cm^2) and air-dried at room temperature. The Pt/C catalyst loading was controlled at 1.15 mg cm^{-2}. To study the catalytic performance, we performed the linear sweep voltammetry (LSV) under a sweep rate of 1 mV s^{-1} with the potentials ranging from 0.05 V to -0.5 V vs. RHE in N$_2$-saturated 1.0 M KOH and 1.0 M PBS solution. All the measured potentials were calibrated to RHE via the Nernst equation (E$_{RHE}$ = E$_{Ag/AgCl}$ + 0.059 pH + 0.197). The double-layer capacitance (C$_{dl}$) was acquired by cyclic voltammetry measurement under the potential windows from 0.2 V to 0.3 V vs. RHE with different scan rates of 10, 20, 40, 60, 80, 100 mV s^{-1}. The C$_{dl}$ is obtained by plotting the j$_a$ - j$_c$ at overpotential of 0.25 V (where j$_a$ and j$_c$ are the anodic and cathodic current densities, respectively) against the scan rate, and the slope is twice that of C$_{dl}$. Chronopotentiometry test was conducted at a constant applied overpotential to check its electrochemical stability. To correct the ohmic drop, the compensated potentials were corrected by the equation $E_{corrected}$ = E_{raw} - IR_s, where R_s was the contact resistance derived from EIS data.[1] All the electrochemical tests were carried out at room temperature.

I.6 Mass activity and Turnover frequency. The values of mass activity (A g^{-1}) were calculated through normalization of the measured current density j (mA cm^{-2}) at -0.15 V (1 M KOH) or -0.20 V (1 M PBS) using the mass (mg cm^{-2}) of the loading catalysts. The number of active sites (n) was determined by CV collected from -0.2 to +0.6 V vs. RHE in PBS solution at the scan rate of 0.05 V s^{-1}. Assuming a one-electron process for both reduction and oxidation, the upper limit of n could be calculated with the equation: $n = Q/2F$, where Q is the cyclic voltammetric

charge capacity obtained by integrating the CV cures, F is the Faradic constant (96485 C mol^{-1}). The turnover frequency (TOF, s^{-1}) values are calculated [2]via the following equation: TOF= $|j|A/2Fn$, where $|j|$ is the current density at a fixed voltage during the LSV test, A stands for the area of the electrode and n is the numbers of active sites (mol).

I.7 Computational Calculation. All computational calculations were carried out using the Vienna ab initio simulation packages.[3] The generalized gradient approximation with the Perdew-Burke-Ernzerhof exchange-correlation functional was used in the description of the exchange and correlation interactions with a energy cut off of 520 eV.[4-5] The k-points were sampled on basis of the Monkhorst-Pack method.[6] To minimize the undesired interactions between images, a vacuum of at least 15 Å was considered along the z axis. The convergence threshold was set as 10^{-5} eV in energy and 0.02 eV/Å in force.[6] DFT simulations performed were based on the experimentally crystal structure of NiS_2 (JCPDS No. 88-1709; space group: *Pa-3*, $a = b = c = 5.687$ Å). Calculations of the H and H_2O adsorption free energetics were performed on the (001) surface, which is most common surface for pyrite.[7] A supercell containing (2×2) NiS_2 (001) slab and at least 15 Å vacuum space was used in the calculations. The Mn-doped model of NiS_2 slab was established based on the NiS_2 (001) surface by substituting two Ni atoms with Mn atoms. The formation energy was calculated as: E_f= E(Mn-NiS_2) – E(NiS_2) + $2\mu_{Ni}$ – $2\mu_{Mn}$, where E(Mn-NiS_2) and E(NiS_2) are the total energies of Mn-doped NiS_2 and pure NiS_2, respectively, and μ is the chemical potential of Ni or Mn. The H and H_2O/OH adsorption were studies to provide theoretical poof for the HER performances. The H adsorption energy was calculated relative to H_2 (g) using this equation: ΔE = E(slab+H) – E(slab) – 1/2E(H_2). The Gibbs free energy (ΔG_H) is shown in the following equation: ΔG_H = ΔE_H + ΔZPE – TΔS, where ΔZPE and ΔS are the zero-point energy change and the entropy change of H adsorption, receptivity. Since ΔZPE – T$\Delta S \approx 0.24$ eV,[8] we have ΔG_H =ΔE_H + 0.24 eV.
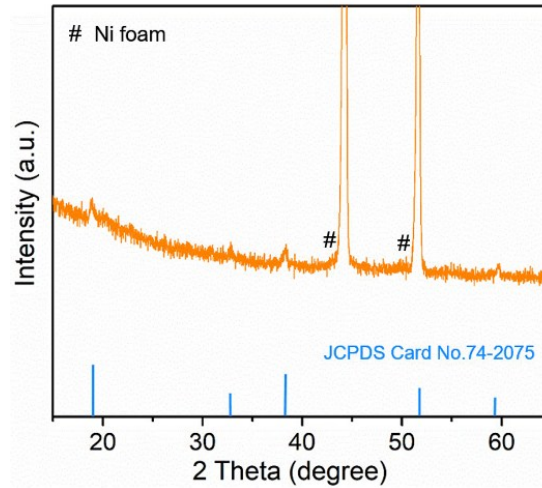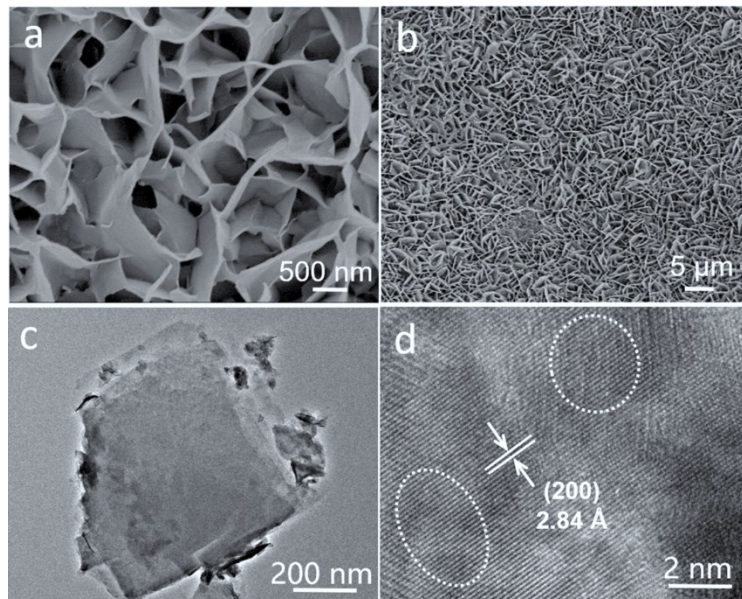
II Additional Figures and Tables
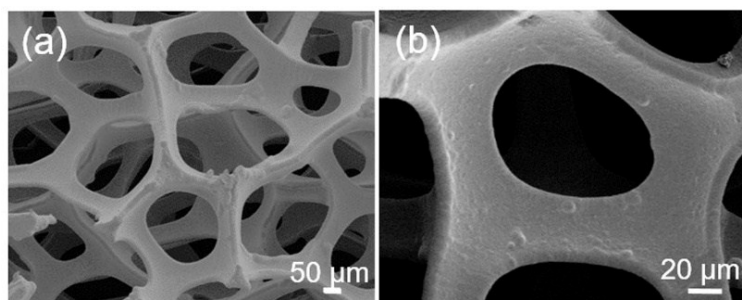
Figure S1. SEM images of bare Ni foams with different magnifications.
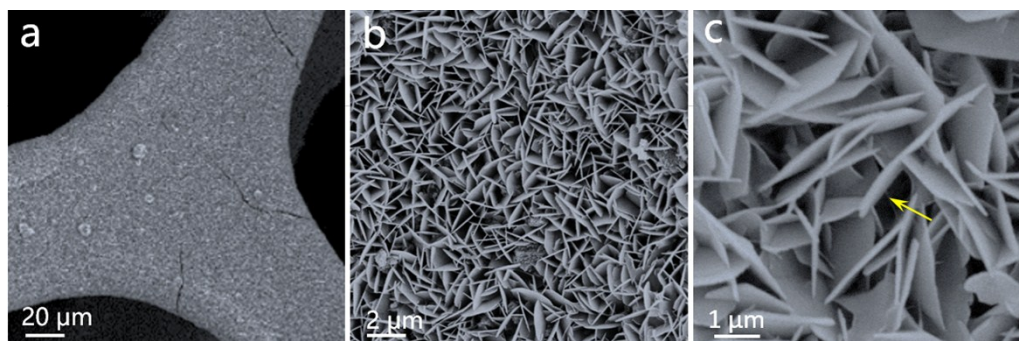

Figure S2. SEM images with different magnifications of Mn-Ni hydroxide precursor. The yellow arrows in (c) indicates the void spaces between the interconnecting nanosheets.
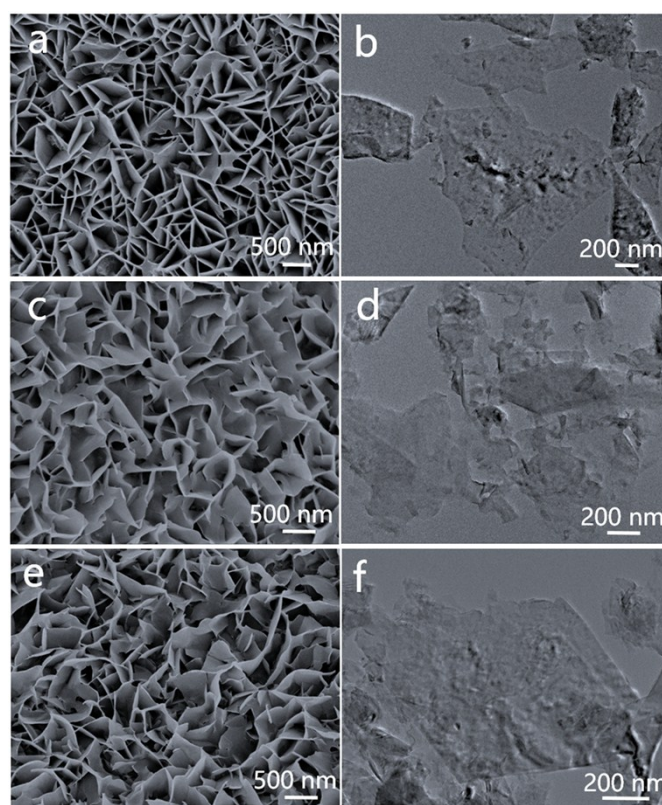
**Figure S3.** XRD pattern of Mn-Ni hydroxide precursor.

Figure S4. (a, b) SEM images of with different magnifications. (c) TEM image. (d) HRTEM image for the pure NiS_2/NF. White dotted circles in (d) indicate the regular lattice structure in the bare NiS_2 nanosheet.
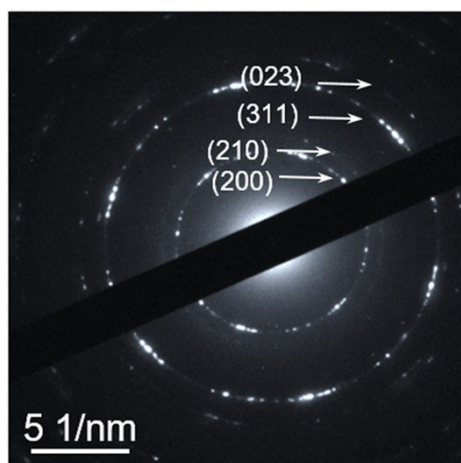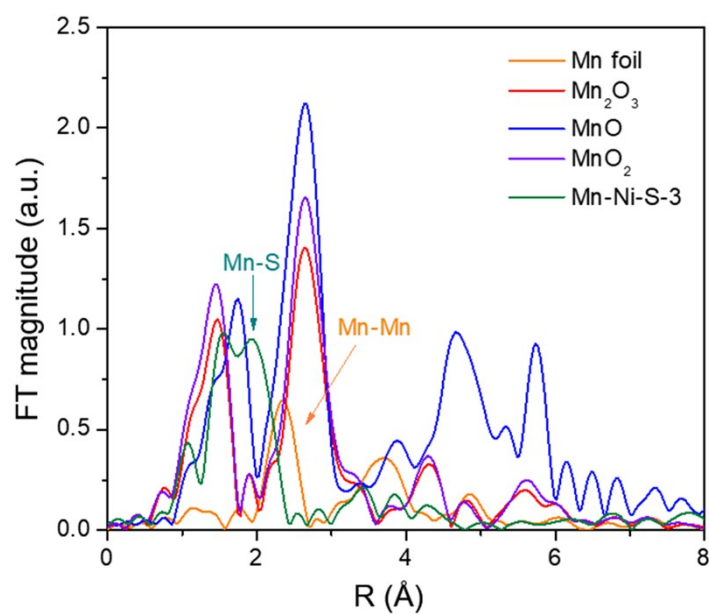
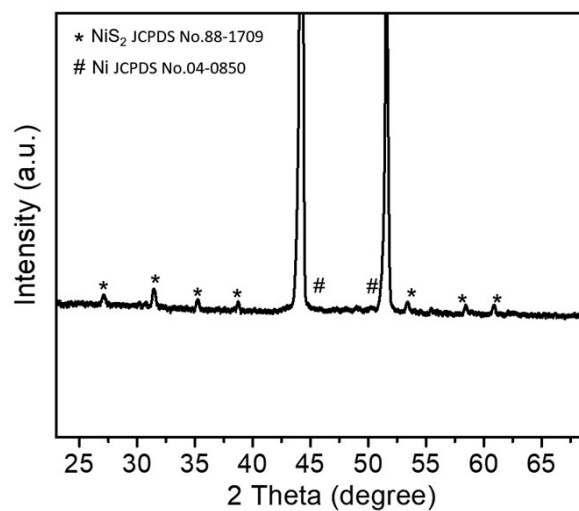**Figure S5.** The SAED image of Mn-Ni-S/NF-3 nanosheet.

Figure S6. (a, c, e) SEM images and (b, d, f) TEM images for (a, b) Mn-Ni-S/NF-1 (3.5 atom % Mn), (c, d) Mn-Ni-S/NF-2 (6.5 atom % Mn), and (e, f) Mn-Ni-S/NF-4 (11 atom % Mn).
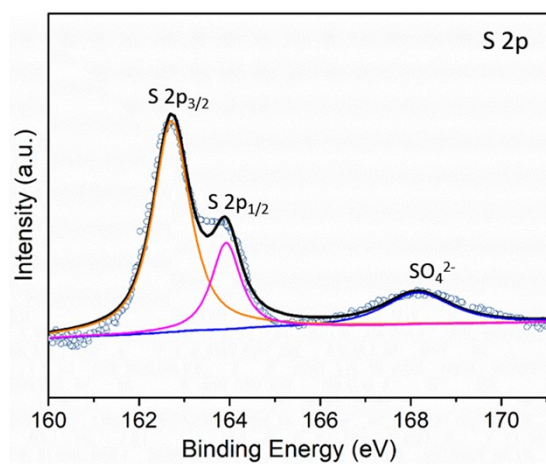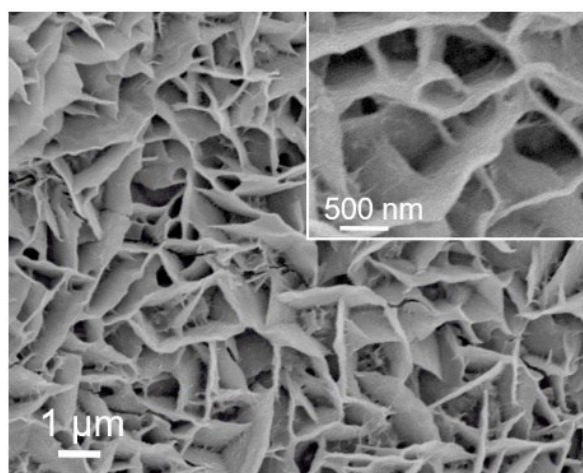
Figure S7. XPS spectra of S 2p for Mn-Ni-S-3 nanosheets.
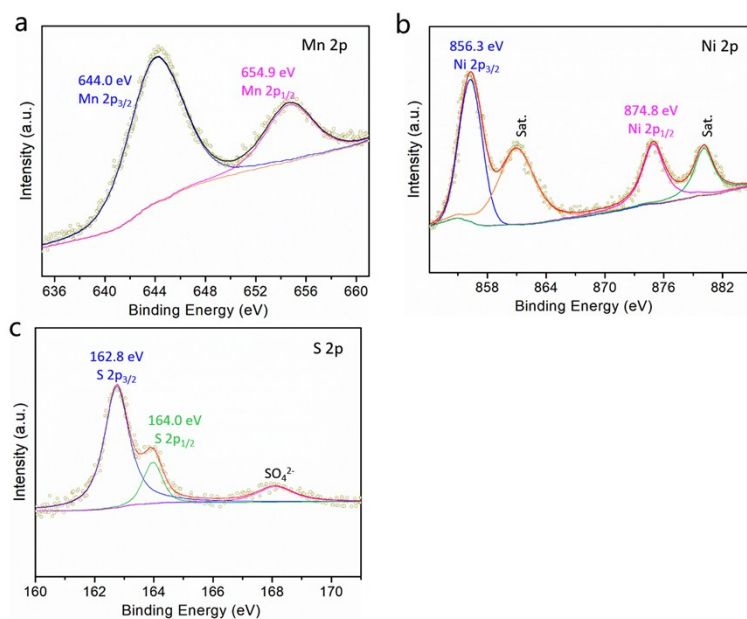

Figure S8. FT Mn K-edge at *R* space of Mn foil, Mn$_2$O$_3$, MnO and Mn-Ni-S-3.

Figure S9. XRD pattern of Mn-Ni-S/NF-3 after long-term HER electrolysis.
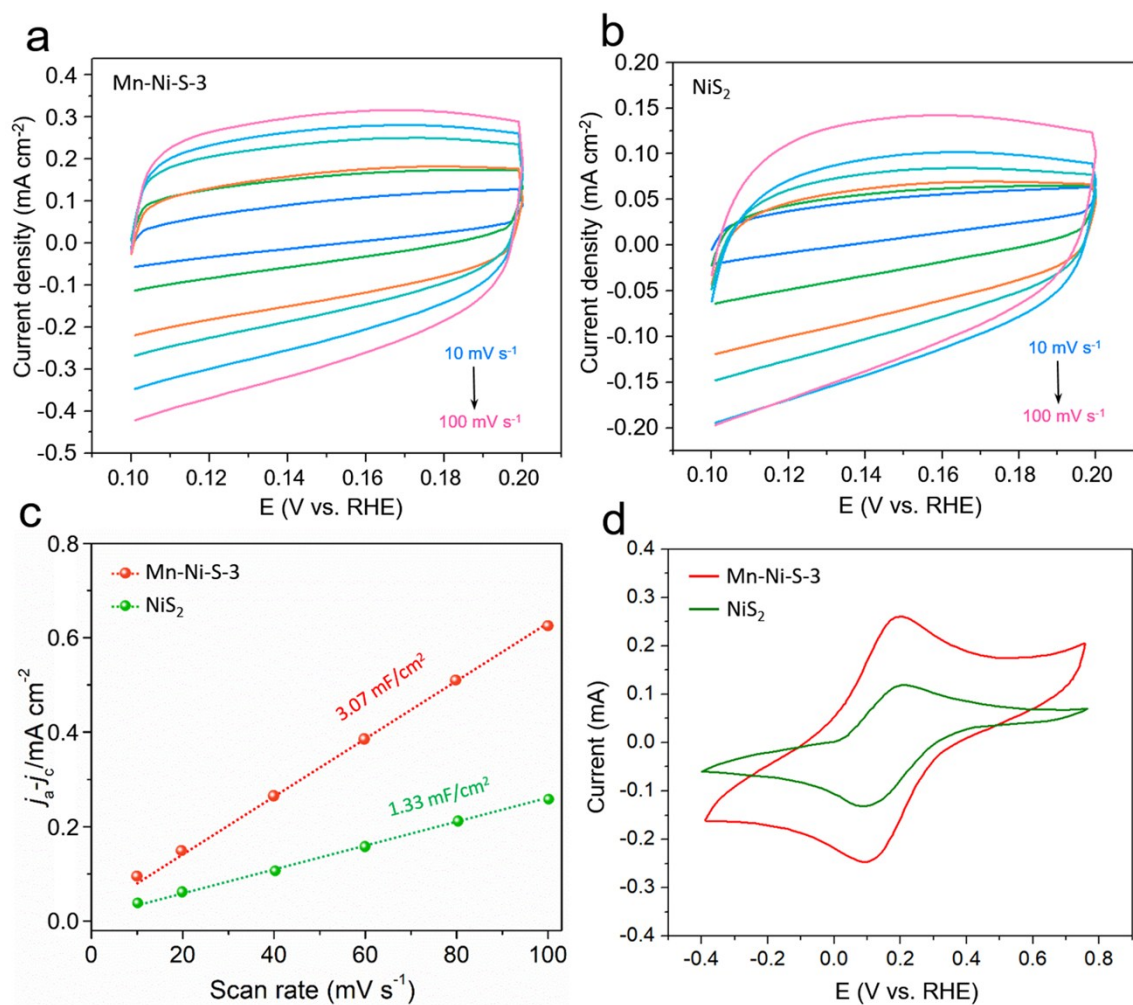

Figure S10. SEM images of Mn-Ni-S/NF-3 after long-term HER electrolysis.

Figure S11. XPS spectra of (a) Mn 2p, (b) Ni 2p and (c) S 2p for Mn-Ni-S/NF-3 after long-term HER electrolysis.
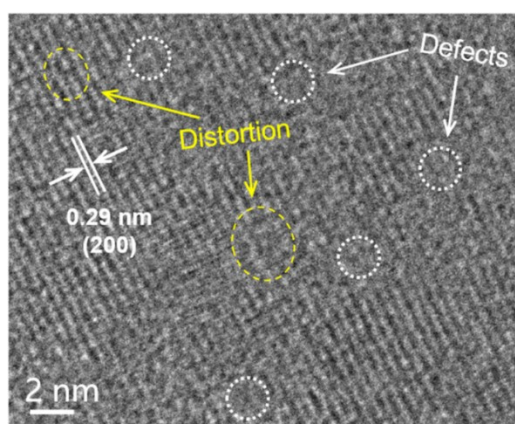
Figure S12. HRTEM image of Mn-Ni-S/NF after HER electrolysis. The while circle refers to the defects, and the yellow circle refers to the lattice distortion.

Figure S13. CV curves in an overpotential windows of 0.10-0.20 mV vs. RHE for (a) Mn-Ni-S-3/GCE and (b) NiS_2/GCE. (c) Charging current density differences at different scan rates. (d) CVs of 0.01 M $Fe(CN)_6^{3-}/^{4-}$ in 1 M KCl using different catalysts casted on GCE.
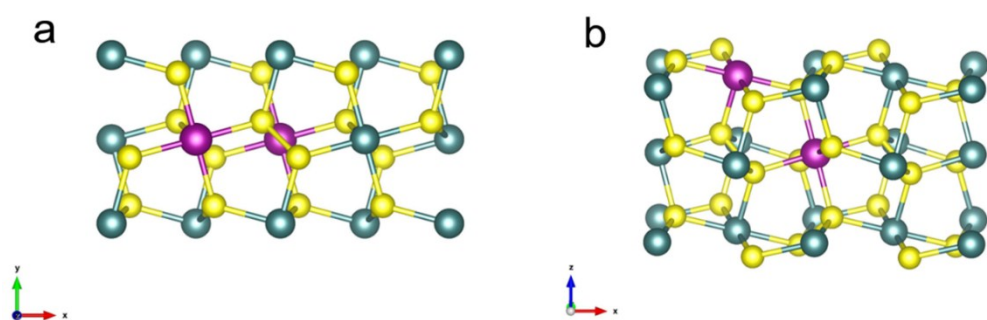
Figure S14. (a) Top and (b) side view of the Mn-doped NiS_2 (001) surface by substituting two Ni atoms with Mn atoms.
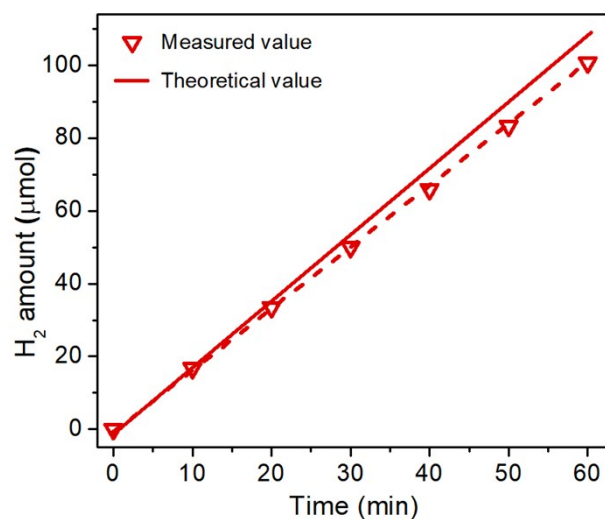
Figure S15. The faradaic efficiency of the doped Mn-Ni-S/NF electrode toward HER in seawater at the overpotential of 400 mV.

Table S1. Mn/Ni feed ratio and atomic ratio for Mn-Ni-S/NF with various Mn content.

Sample	$MnSO_4 \cdot H_2O/Ni(NO_3)_2 \cdot 6H_2O$ feed ratio (mmol/mmol)	Mn/Ni ratio of catalysts from ICP (mg/mg)	Mn-doped NiS_2/NF (atomic ratio: Mn/Mn+Ni)
1	0.10 / 1.90	0.0272 / 0.794	3.5%
2	0.15 / 1.85	0.0355 / 0.545	6.5%
3	0.20 / 1.80	0.0635 / 0.685	9%
4	0.25 / 1.75	0.0724 / 0.625	11%

Table S2. Summary of representative recently reported earth-abundant HER electrocatalysts in alkaline electrolyte

Catalysts	Support	Mass loading (mg cm^{-2})	η (mV) at 10 mA cm^{-2}	Tafel slope (mV dec^{-1})	TOFs (s^{-1})	Mass activity@150 mV (A g^{-1})	Reference
Mn-doped NiS$_2$	Ni Foam	1.15	71	57	1.02@100 mV	71.5	*This work*
Co-Mo/Ti	Ti foil	1.0	75	58	—	55	*J. Mater. Chem. A* 2016, **4**, 3077.
Fe-doped CoP	Ti foil	1.5	78	48	—	~65	*Adv. Mater.* 2017, **29**, 1602441.
WS$_{2(1-x)}$Se$_{2x}$/NiSe$_2$	Ni Foam	5.4	78	68	—	~35	*Nano Lett.* 2016, **16**, 7604.
Cr-doped FeNi-P	Glassy carbon	0.48	190	106.5	0.214@100 mV	~15	*Adv. Mater.,* 2019, **31**, e1900178.
Amorphous NiFeP	Ni Foam	~1.8	158	122	0.36@250 mV)	~5	*ACS Energy Lett.,* 2016, **2**, 1035-1042.
Co-Ni$_3$N	Carbon cloth	2.91	195	156	0.146@290 mV	~20	*Adv. Mater.,* 2018, **30**, e1705516.
N, P-MoS$_2$	Carbon cloth	1.2	78	113	0.58@200 mV	41.6	*Nano Energy,* 2019, **58**, 862-869.
Ni-CoP	Glassy carbon	—	90	71	0.1@164 mV	—	*Nano Energy,* 2019, **56**, 411-419.
CoSe/Ti	Ti foil	1.2	121	65	—	~5	*Chem. Commun.* 2018, **51**, 16683.
NiCoP nanotubes/NF	Ni Foam	1.8	150	80	—	5	*Adv. Funct. Mater.* 2016, **26**, 6785.
MoS$_2$-Ni$_3$S$_2$ nanoparticles/NF	Ni Foam	13	145	62	—	~3	*ACS Catal.* 2017, **7**, 2357.
CoO$_x$@CN	Glass carbon	1.78	234	85	—	~3	*J. Am. Chem. Soc.* 2015, **137**, 2688.

Table S3. Summary of representative recently reported HER electrocatalysts in neutral electrolyte

Catalysts	Support	Mass loading (mg cm^{-2})	η (mV) at 10 mA cm^{-2}	Tafel slope (mV dec^{-1})	Mass activity@200 mV (A g^{-1})	Reference
Mn-doped NiS$_2$	**Ni Foam**	**1.15**	**84**	**65**	**56.5**	*This work*
CoP nanowire/CC	Carbon choth	0.92	106	93	~24	*J. Am. Chem. Soc.* 2014, **136**, 7587.
MoP$_2$ NS/CC	Carbon choth	2.8	85	70	9.2	*J. Mater. Chem. A* 2016, **4**, 7169.
Ni-doped FeP /CFP	Carbon paper	0.8	117	72	~50	*Sci. Adv.* 2019, **5**, eaav6009.nb
WP nanorod/CC	Carbon choth	1.5	200	125	~15	*ACS Appl. Mater. Inter.* 2014, **6**, 21874.
MoS$_2$/Ti plate	Ti plate	1.5	200	152	22	*Electrochim. Acta* 2015, **168**, 256.
FeP NAs/NF	Glass carbon	—	202	71	—	*ACS Catal.* 2014, **4**, 4065.
CoP NS/NF	Ni Foam	2.0	149	58	~35	*Chem. Mater.* 2014, **26**, 4326.
WP NAs	Glass carbon	1.5	202	71	~10	*ACS Appl. Mater. Inter.* 2017, **6**, 21874.
FeP/CC	Carbon choth	—	90	115	—	*ACS Appl. Mater. Inter.* 2014, **6**, 20579.
Amorphous Co-S film	FTO	1.5	160	93	~15	*J. Am. Chem. Soc.* 2013, **135**, 17699.
Co-C-N complex	Glass carbon	1.25	107	273	~10	*J. Am. Chem. Soc.* 2015, **137**, 15070.
CoP-MNA/NF	Ni foam	1.92	189	180	~14	*Adv. Funct. Mater.* 2018, **25**, 7337.
3D MoS$_2$/N-GAs	Glass carbon	1.7	261	230	8.8	*J. Mater. Chem. A* 2014, **2**, 13795.
NiSe@NC	Ni foam	—	170	160	~5	*Nanoscale* 2018, **10**,

Table S4. Comparison of HER activity of Mn-Ni-S/NF with other previously reported Ni- or Mo-based electrocatalysts under seawater.

Sample	mass loading (mg cm^{-2})	η vs. RHE (mV) @j=10 mA cm^{-2}	References
Mn-Ni-S/Ni foam	1.15	301	This work
NP-MoS$_2$/Carbon clothes	1.2	345	*Nano Energy,* **2019***, 58, 862*
Mo$_2$C-MoP NPC/CFP	—	346	*Electrochim. Acta.* **2018***, 281*, 710
CoMoP@C/Carbon paper	0.354	~510	*Energy Environ. Sci.* **2017***, 10*, 788
Ni-Mo-S/ Carbon clothes	0.96	~1070	*Sci. Adv.* **2015***, 1*, e1500259

References

[1] H. Liang, A. N. Gandi, D. H. Anjum, X. Wang, U. Schwingenschlögl, H. N. Alshareef, *Nano Lett.* **2016**, 16, 7718.

[2] K. Sun, L. Zeng, S. Liu, L. Zhao, H. Zhu, J. Zhao, Z. Liu, D. Cao, Y. Hou, Y. Liu, Y. Pan, C. Liu, *Nano Energy* **2019**, 58, 862.

[3] G. Kresse, J. Furthmüller, *Phys. Rev. B* **1996**, 54, 11169.

[4] J. P. Perdew, K. Burke, M. Ernzerhof, *Phys. Rev. Lett.* **1996**, 77, 3865.

[5] S. Grimme, *J. Electrochem. Soc.* **2006**, 27, 1787.

[6] M. Desjarlais, J. Kress, L. Collins, *Phys. Rev. E* **2002**, 66, 025401.

[7] J. Hao, W. Yang, J. Hou, B. Mao, Z. Huang, W. Shi, *J. Mater. Chem. A* **2017**, 5, 17811.

[8] J. K. Nørskov, T. Bligaard, A. Logadottir, J. Kitchin, J. G. Chen, S. Pandelov, U. Stimming, *J. Electrochem. Soc.* **2005**, 152, J23.